Planet 1

Asymmetric Dust Distributions in Debris Disks and Their Impact on the Direct Imaging of Earth-Mass Exoplanets

Flux ratio of dust emission to central starlight

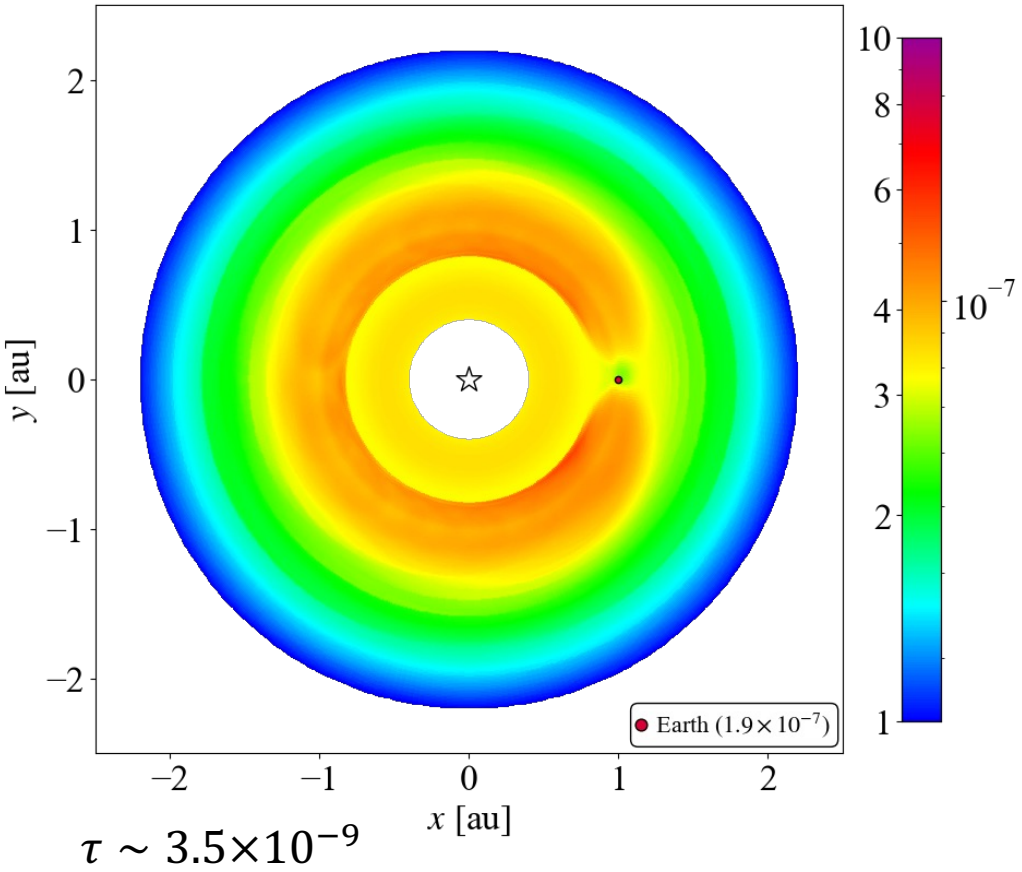

Hayato Shimizu[1]

Collaborator: Hiroshi Kobayashi[1]

[1]Nagoya University

Overview

- Simulate the spatial distribution of dust
- Study the brightness of dust disks around planets

Observation of Exoplanets

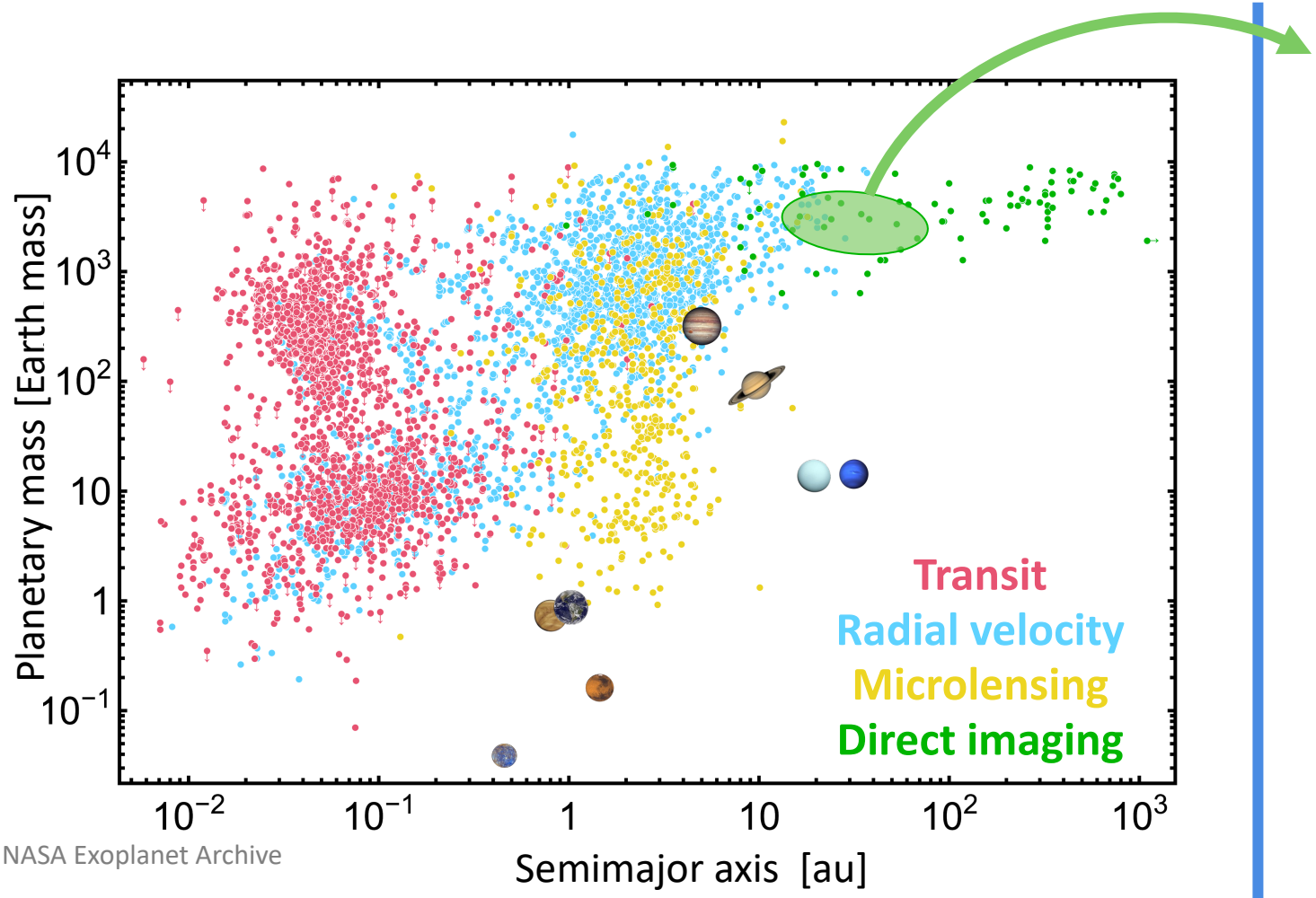

NASA Exoplanet Archive

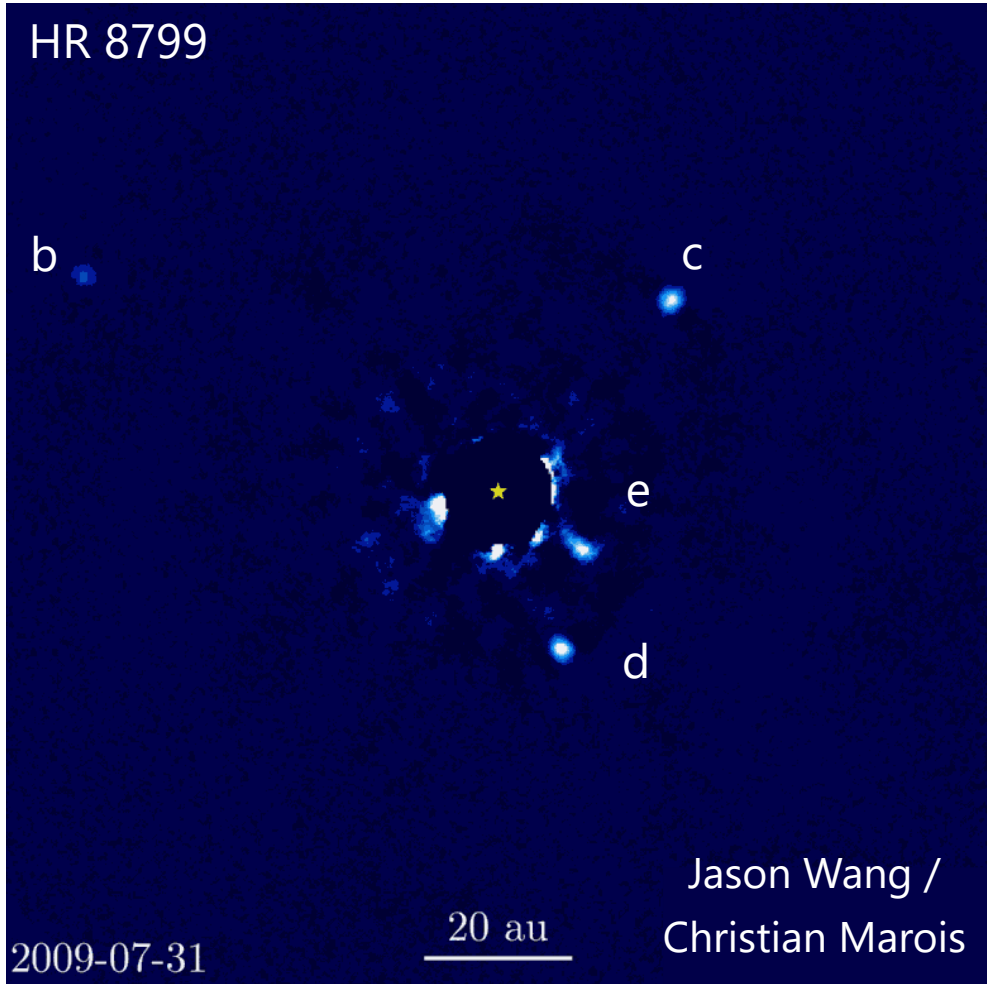

Dust Effects on Direct Imaging

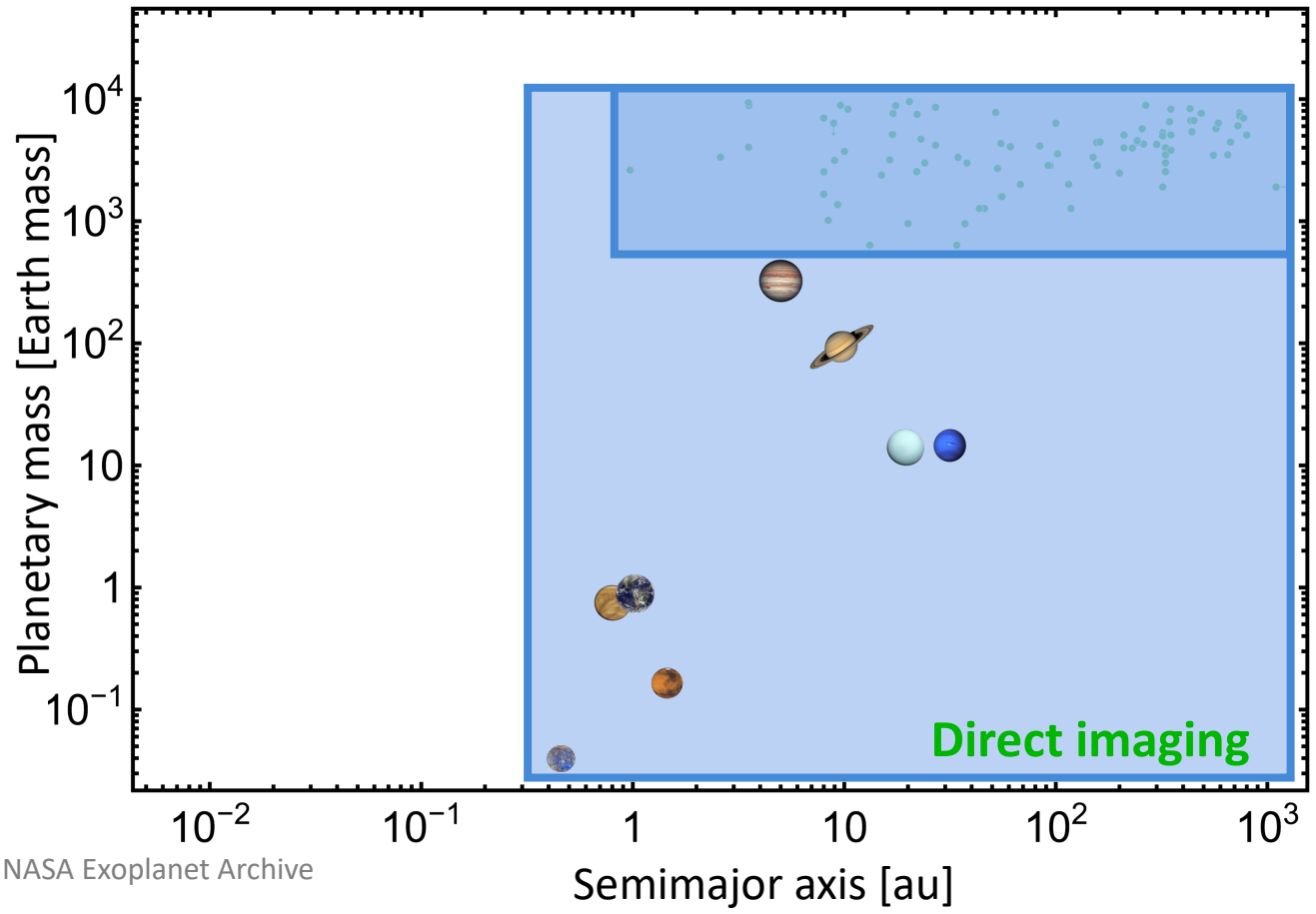

NASA Exoplanet Archive

In the future, it will be possible to directly image fainter terrestrial planets inside the Jupiter-type planets.

The spatial distribution of dust around planets is important.

Dust thermal radiation from planets
Will it interfere with direct imaging?

Characteristic dust structure
Does it suggest the existence of a planet?

→ Investigating the dust flux distribution in **thin** debris disks around terrestrial planets.

Procedure for Determining Dust Flux Distribution

Step 1 Calculate the dust orbits

Step 2 Obtain the surface density distribution

Step 3 Compute the flux of a steady-state dust disk

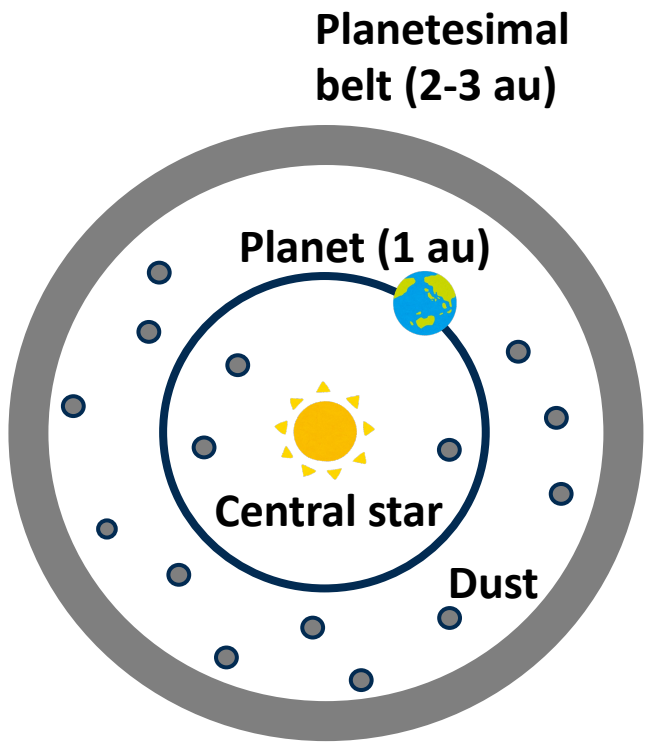

Does a thin debris disk make it **easier** or more **difficult** to detect planets?

Step 1. Calculate the Dust Orbit by Hermite Scheme

- Solve the three-body problem of a central star, planet, and dust.
- Equation of dust motion around the central star (Burns et al. 1979).

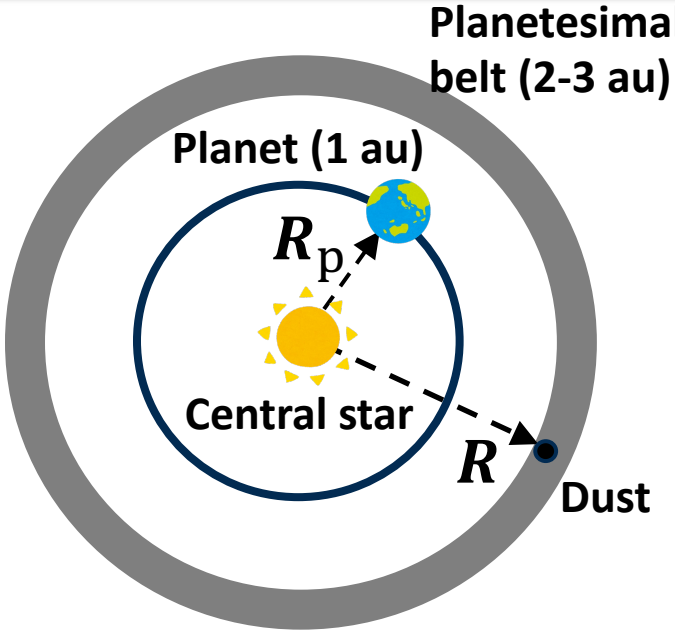

Gravity of the central star, **Radiation pressure** **Planetary gravity**

$$\frac{\mathrm{d}^2\boldsymbol{R}}{\mathrm{d}t^2} = -GM_\star(1-\beta)\frac{\boldsymbol{R}}{|\boldsymbol{R}|^3} - GM_\mathrm{p}\left(\frac{\boldsymbol{R}-\boldsymbol{R}_\mathrm{p}}{|\boldsymbol{R}-\boldsymbol{R}_\mathrm{p}|^3} + \frac{\boldsymbol{R}_\mathrm{p}}{|\boldsymbol{R}_\mathrm{p}|^3}\right)$$

$$-\frac{GM_\star\beta_\mathrm{PR}}{c|\boldsymbol{R}|^2}\left(\frac{\boldsymbol{V}\cdot\boldsymbol{R}}{|\boldsymbol{R}|}\frac{\boldsymbol{R}}{|\boldsymbol{R}|} + \boldsymbol{V}\right)$$

Poynting-Robertson effect (P-R effect)

Ratio of **radiation pressure** to **gravity**

$$\beta = \frac{L_\star r_\mathrm{dust}^2}{4|\boldsymbol{R}|^2 c} \Big/ \frac{GM_\star m_\mathrm{dust}}{|\boldsymbol{R}|^2}$$

$$\propto 1/r_\mathrm{dust}$$

Inversely proportional to dust radius

β	0.2	0.063	0.02	0.0063	0.002
r_dust [μm]	1.43	4.53	14.3	45.3	143
Size	Small				Large

Step 1. Results

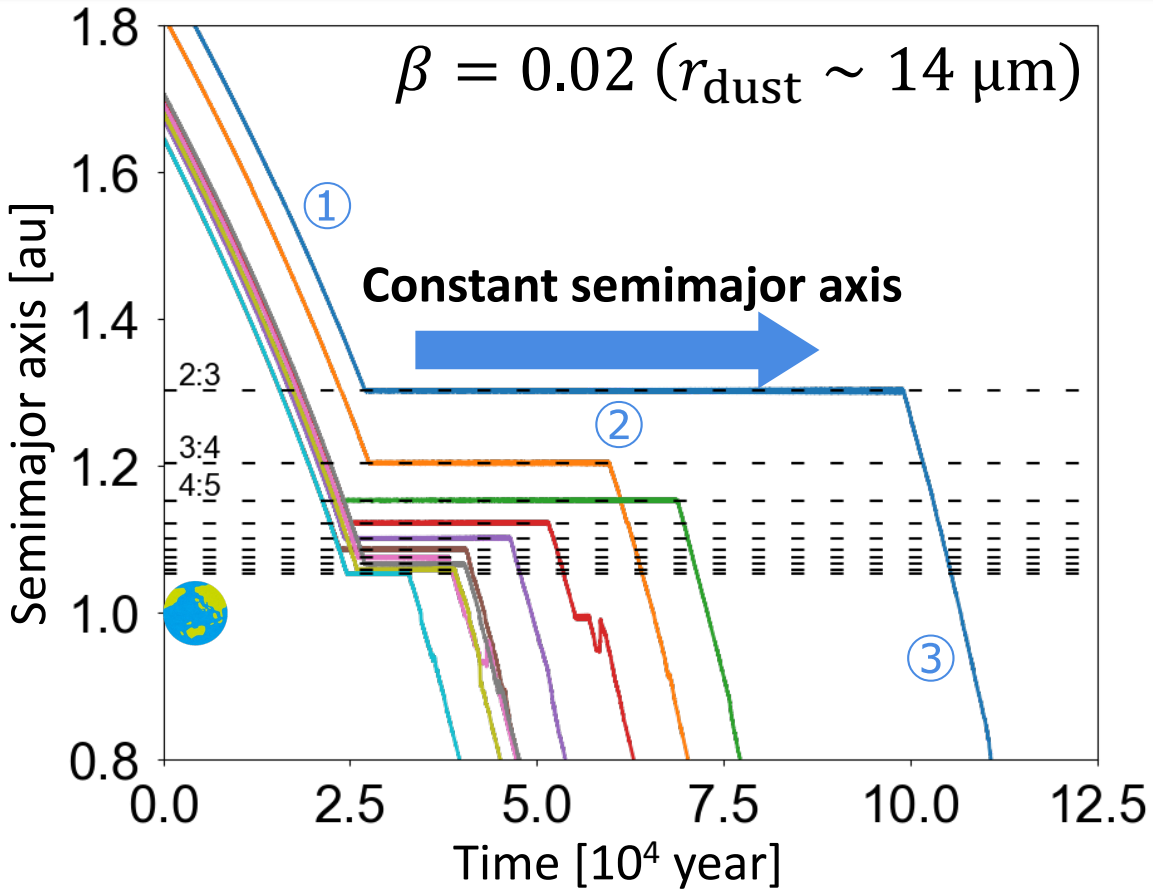

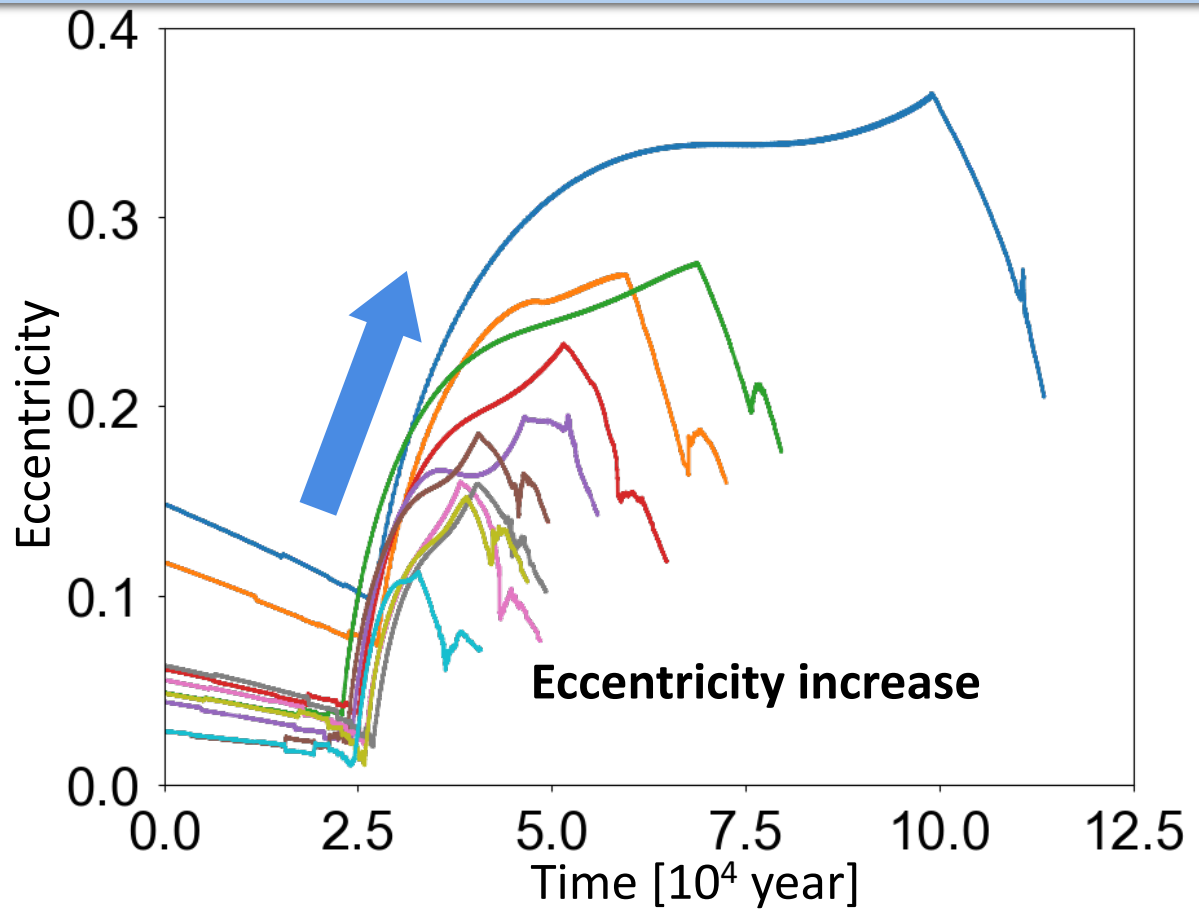

①**Falling** in a spiral orbit, ②**Captured** in a mean motion resonance, ③**Escape** resonance.

The capture location and capture time depend on β and initial conditions.

Step 2. Obtain the Surface Density Distribution

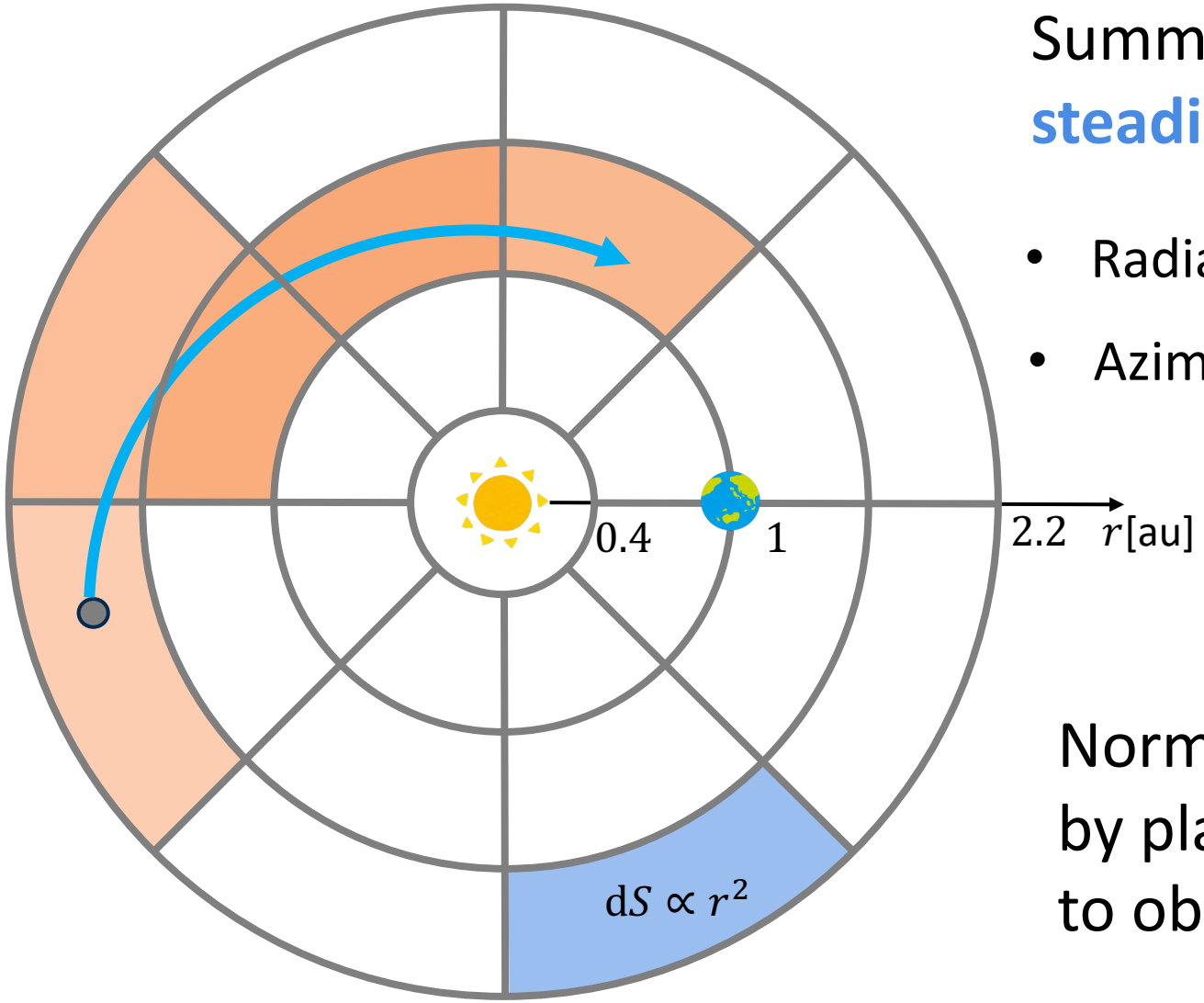

Summing the residence time of dust particles **steadily** arriving from the planetesimal belt

- Radial direction：0.4 – 2.2 au divided into 345 parts
- Azimuthal direction： divided into 360 equal parts

Divide by the area of each region $\mathrm{d}S$ to obtain the surface density.

Normalized relative to the region unaffected by planetary influence ($r = 0.4$ au) to obtain relative surface density.

Step 2. Results

β	0.2	0.063	0.02	0.0063	0.002
r_{dust}	1.43 μm	4.53 μm	14.3 μm	45.3 μm	143 μm
Size	Small				Large

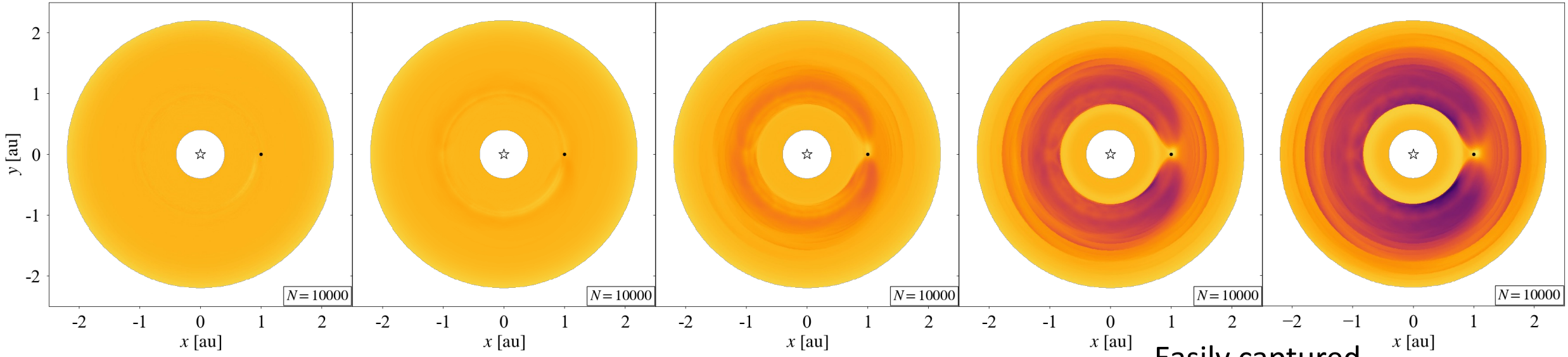

- The **structure varies** depending on the dust size.
- What size is the dust in the debris disk?

Step 3. Calculate Fluxes of Steady-State Dust Disks

Dust is produced in the planetesimal belt.

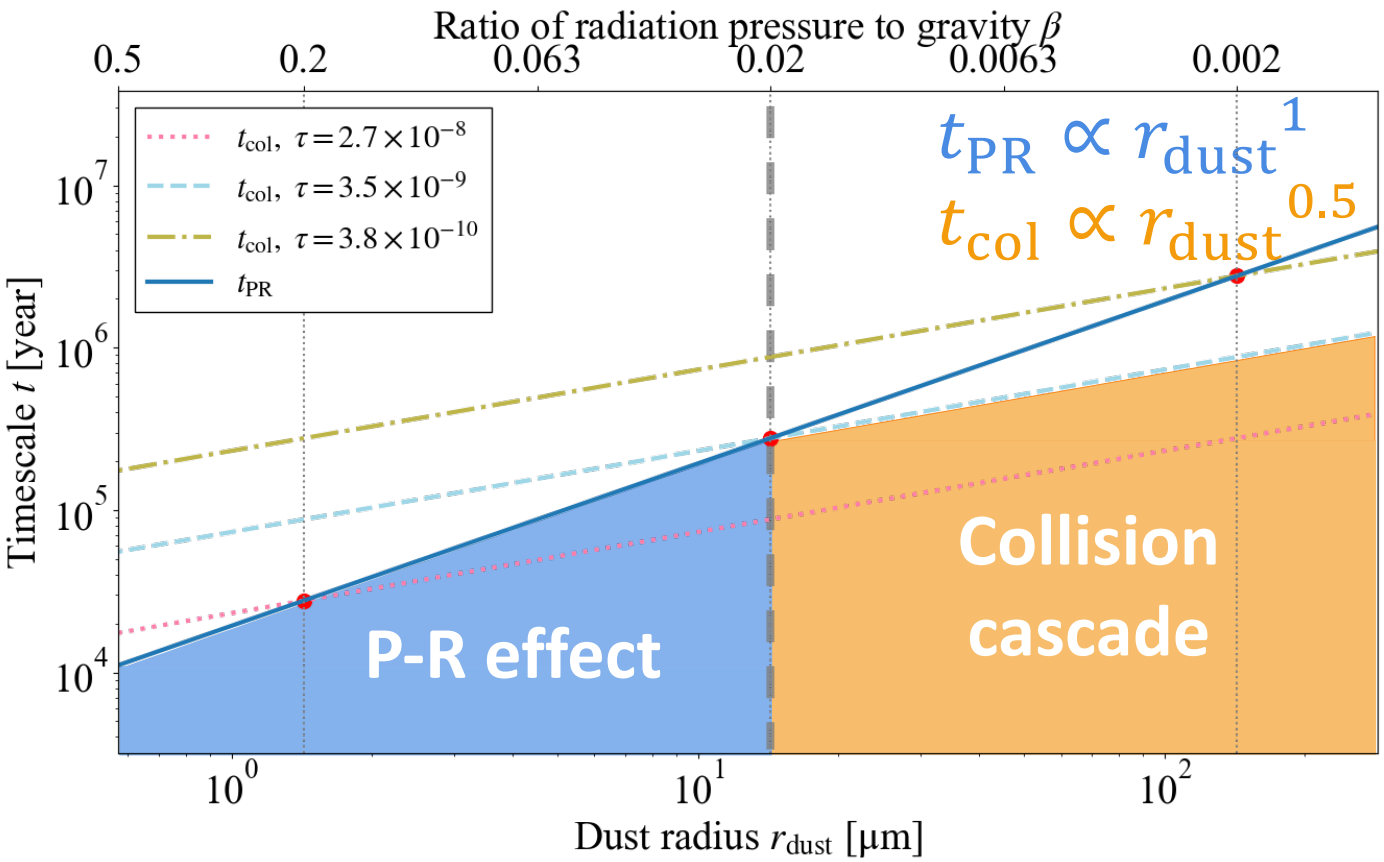

There is a relationship between the **brightness** of the debris disk and the typical dust **size**.

We assume the two power-law size distributions: that is caused by **the collision cascade time** $t_{\rm col} < t_{\rm PR}$, while that is additionally modified by **the P-R effect drift time** $t_{\rm PR} < t_{\rm col}$.

Brightness	Bright	⟷	Faint
Optical thickness τ	2.7×10^{-8}	3.5×10^{-9}	3.8×10^{-10}
Typical dust β	0.2	0.02	0.002

Step 3. Determine Dust Size Distribution

Bright disk

$\tau \sim 2.7\times10^{-8}$

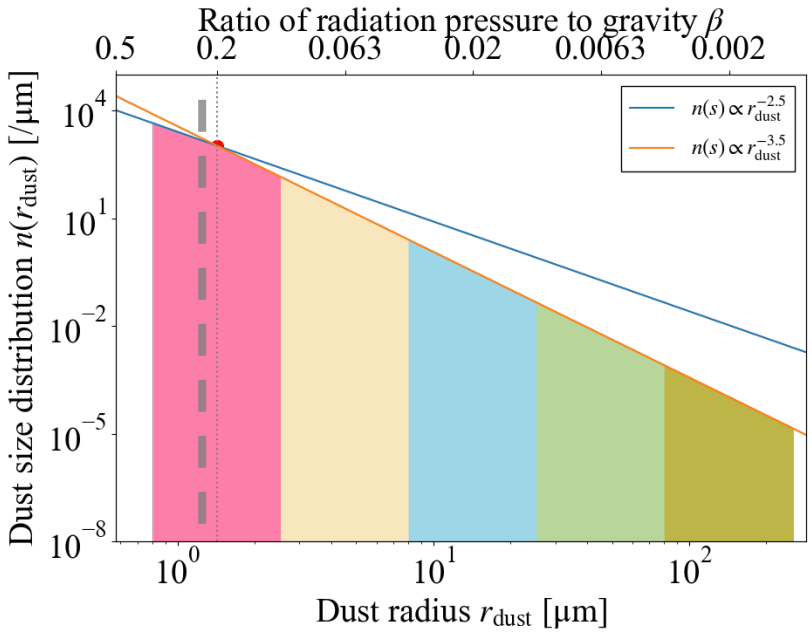

Faint disk

$\tau \sim 3.5\times10^{-9}$

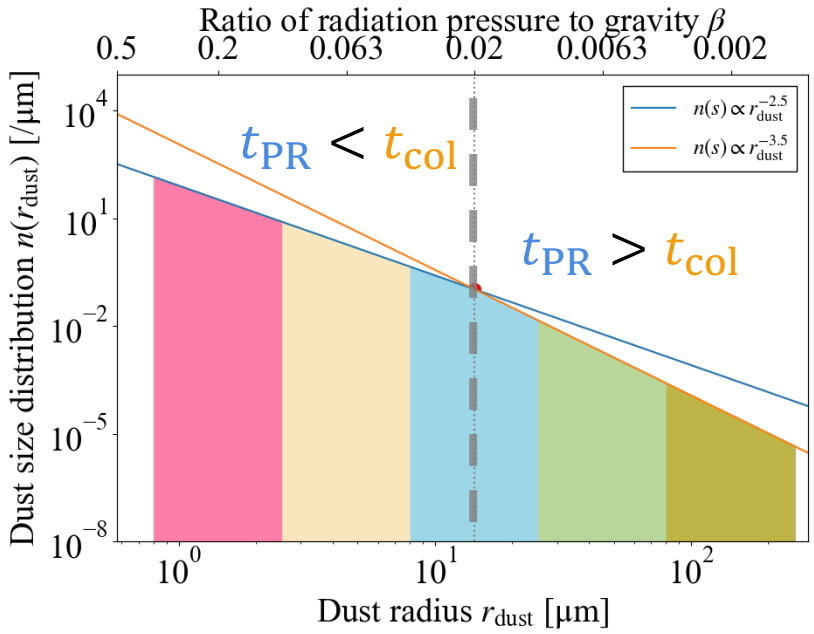

$\tau \sim 3.8\times10^{-10}$

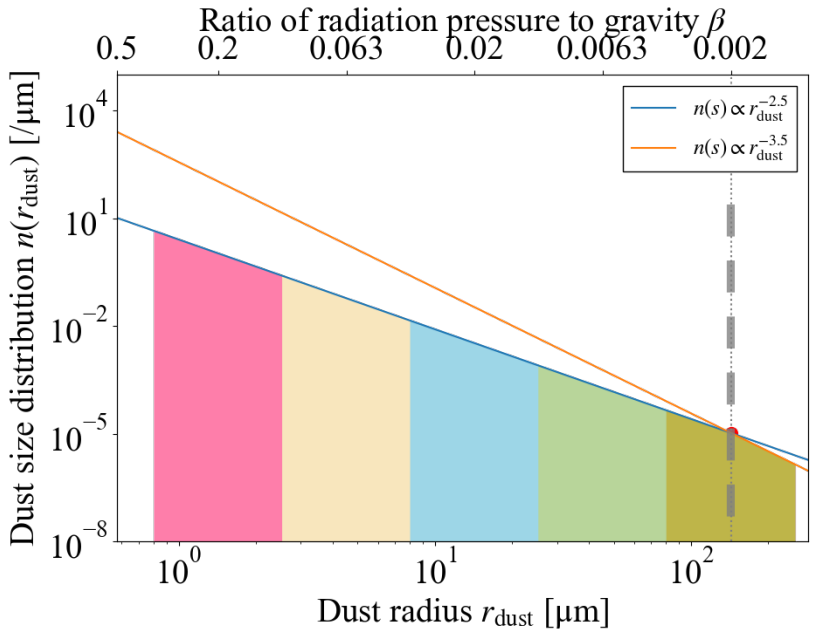

Dust size distribution $n(r_{\rm dust})$

$t_{\rm PR} > t_{\rm col}$ ➡ $n(r_{\rm dust}) \propto r_{\rm dust}^{-3.5}$

$t_{\rm PR} < t_{\rm col}$ ➡ $n(r_{\rm dust}) \propto r_{\rm dust}^{-2.5}$

β	0.2	0.063	0.02	0.0063	0.002
$r_{\rm dust}$ [μm]	1.43	4.53	14.3	45.3	143

Step 3. Results

Wavelength $\lambda = 10\ \mu\mathrm{m}$

Bright disk
$\tau \sim 2.7\times10^{-8}$

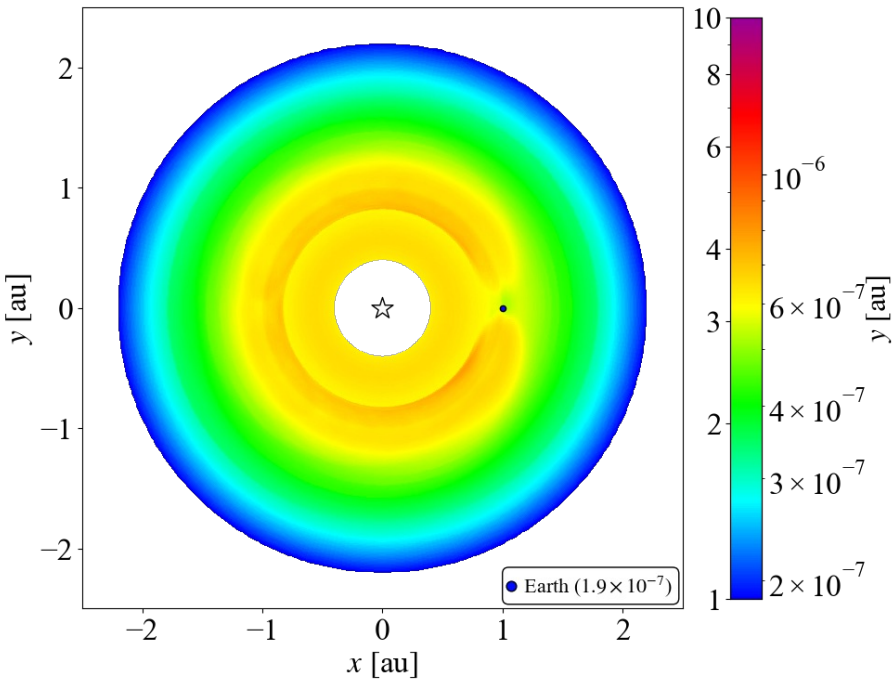

Dust is **thick**, **obscuring** the planet
but revealing **weak** structures

Faint disk
$\tau \sim 3.5\times10^{-9}$

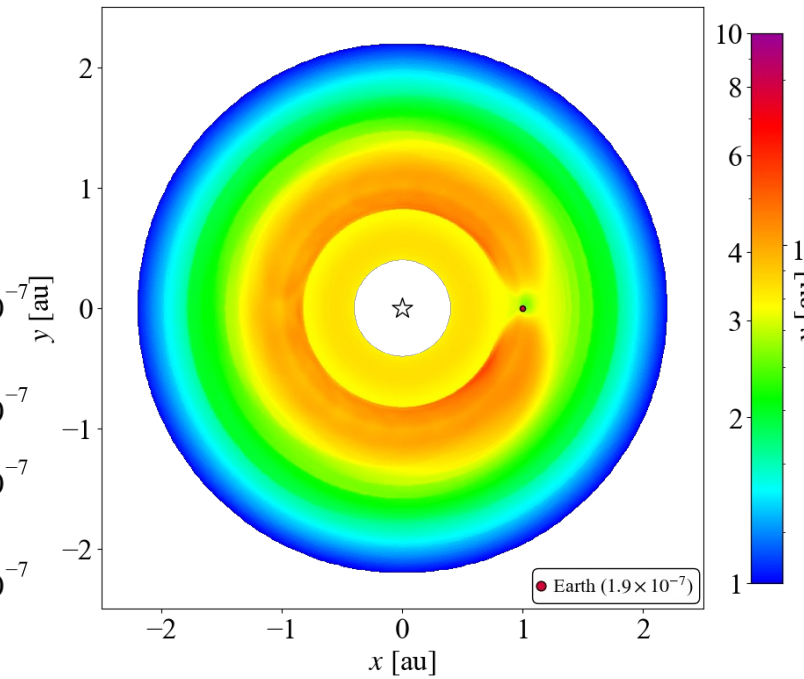

$\tau \sim 3.8\times10^{-10}$

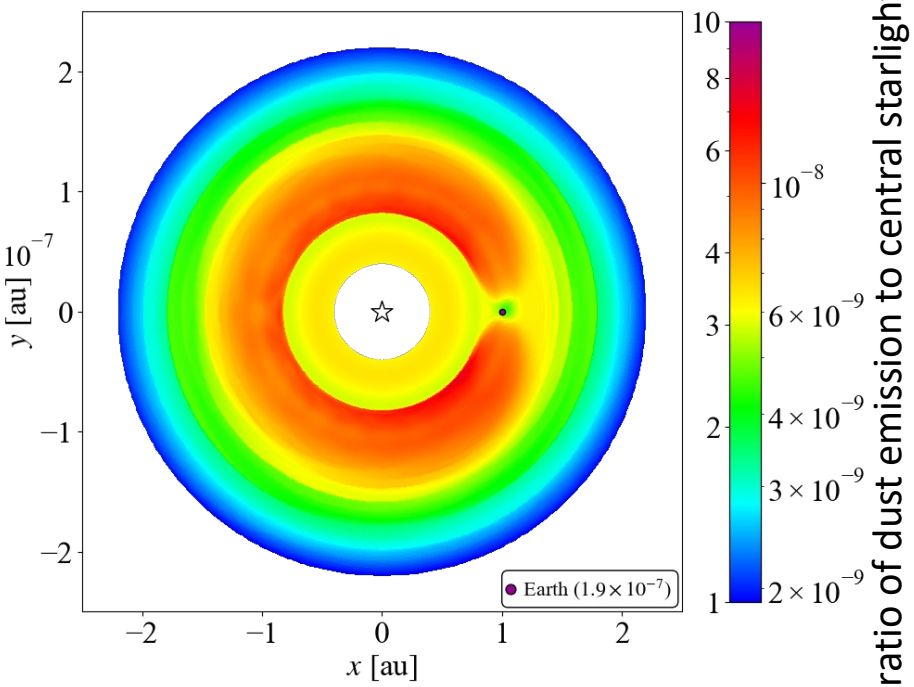

Dust is **thin**, leaving the planet **visible**
while also revealing **strong** structures

Optical thickness τ is small, the **characteristic shapes** are significant.
In faint disks, such **shapes as well as exoplanets** can be observed in future observations.

Summary

- We investigated the structure of steady-state dust disks around planets.
- The **pattern varies** depending on the size of the dust particles.
- The size distribution was derived, and the disk flux was calculated by combining five different sizes. → Optical thickness τ is small, the **characteristic shapes** are significant
- In a faint disk, such **shapes as well as exoplanets** can be observed in future observations.

➡ **Useful** for detecting exoplanets via direct imaging!

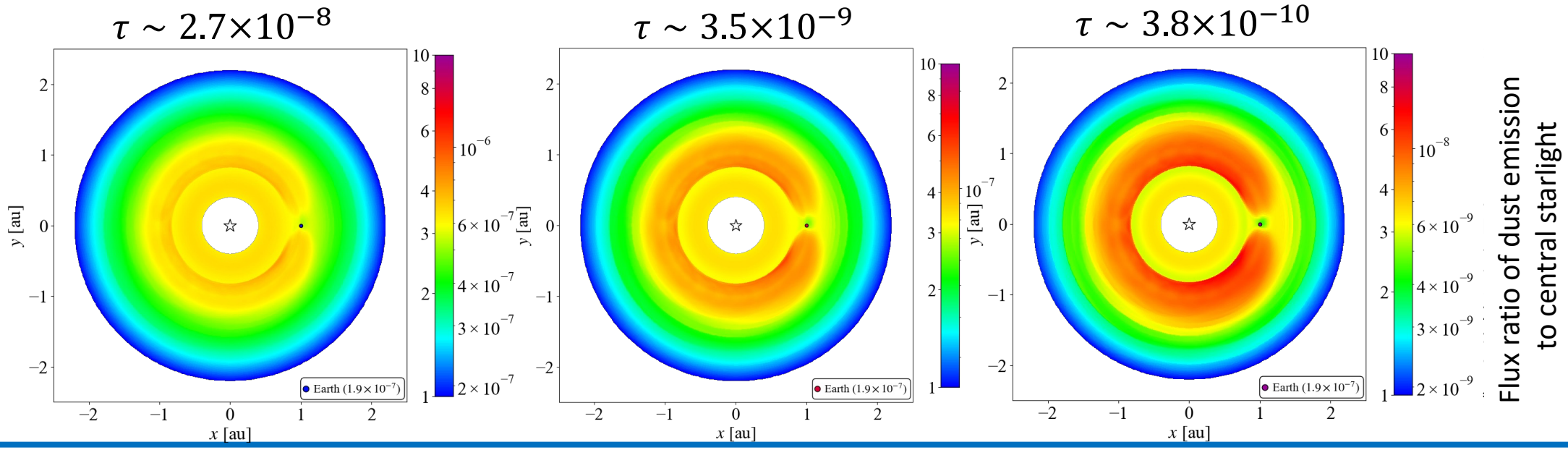

Appendix

Single size disc flux

$\tau \sim 2.7\times10^{-8}$

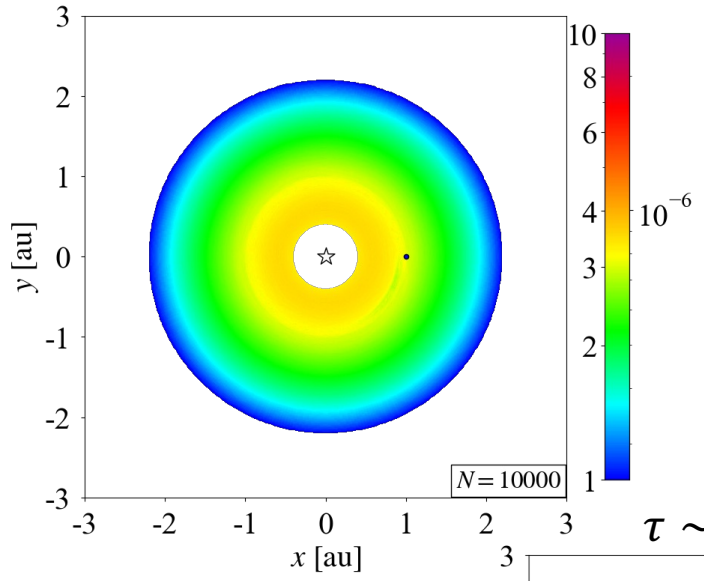

$\tau \sim 3.5\times10^{-9}$

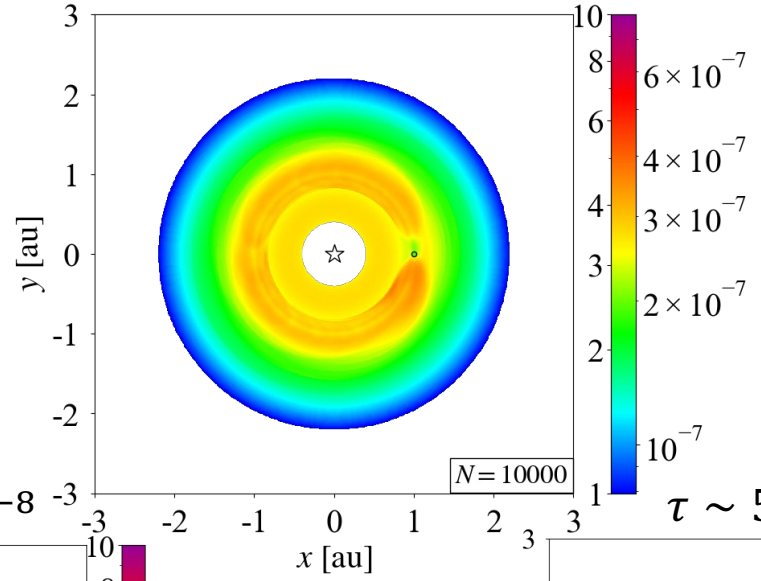

$\tau \sim 3.8\times10^{-10}$

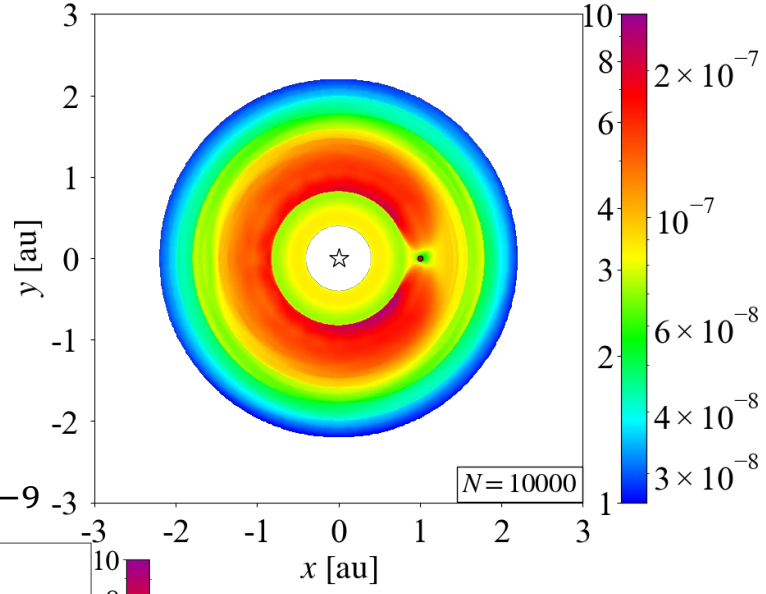

thick disk

$\tau \sim 1.7\times10^{-8}$

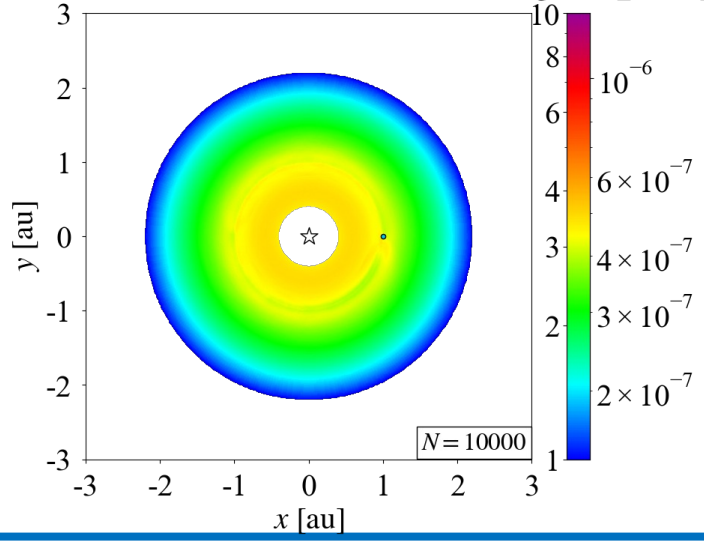

$\tau \sim 5.5\times10^{-9}$

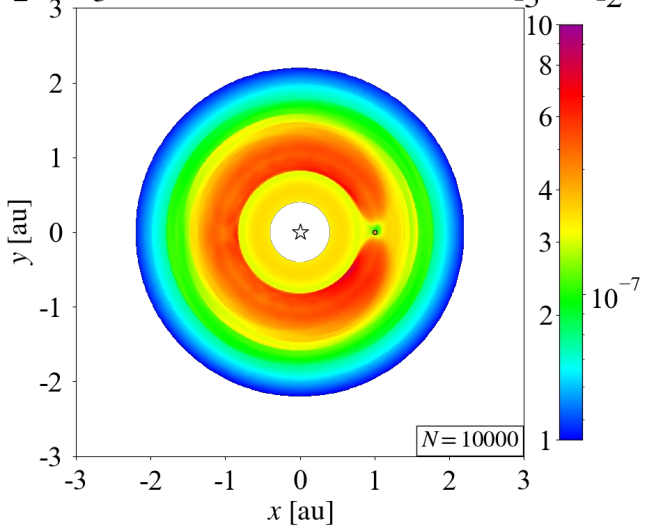

thin disk

Flux Calculation

1 block of dust flux $f_{\mathrm{dust},\nu} = \dfrac{r^2 \tau(r,\phi) B_{\mathrm{dust},\nu}(r,\phi)}{D^2}$

Central star flux $F_{\star,\nu} = \dfrac{\pi R_\star^2 B_{\star,\nu}}{D^2}$

Planck function

$$B_\nu = \frac{2h\nu^3}{c^2} \frac{1}{\exp(\frac{h\nu}{kT}) - 1}$$

dust radiation | Dust absorption of central star radiation

$$4\pi r_{\mathrm{dust}}^2 \sigma T_{\mathrm{dust}}^4 = \frac{\pi r_{\mathrm{dust}}^2}{4\pi r^2} 4\pi R_\star^2 \sigma T_\star^4$$

dust temperature

$$T_{\mathrm{dust}} = 280 \left(\frac{R_\star}{R_\odot}\right)^{\frac{1}{2}} \left(\frac{r}{1\ \mathrm{au}}\right)^{-\frac{1}{2}} \left(\frac{T_\star}{T_\odot}\right) \mathrm{K}$$

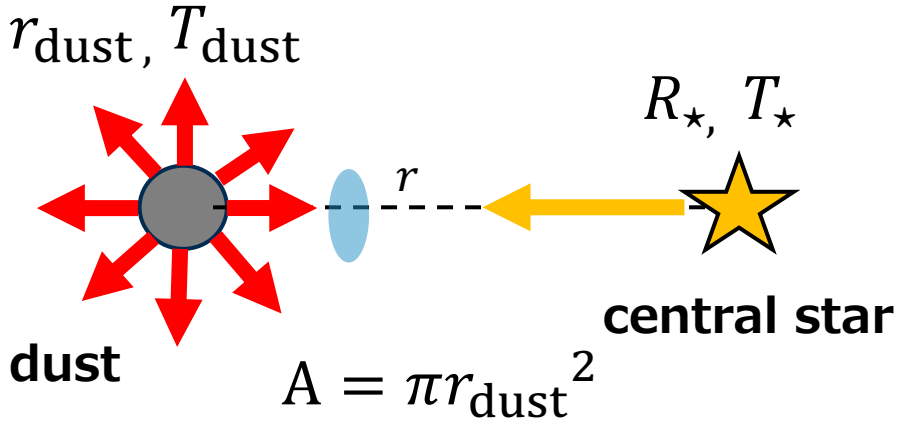

Timescale

$$t_{\rm coll} = \tau_{\rm dep} = \frac{36\, m_{\rm max}^{\frac{1}{3}}}{\Sigma_0 h_0 \Omega_{\rm K}} \left(\frac{v^2}{2Q_{\rm D}^{\star}}\right)^{-\frac{5}{6}} \left[\left(-\ln\epsilon + \frac{1}{2-b}\right)s_1 + s_2 + s_3\right]^{-1}$$

Kobayashi & Tanaka 2010

$$t_{\rm PR} = \frac{a}{v_{\rm r}} = \frac{ca^2}{2\beta_{\rm PR} G M_{\star}} \qquad \frac{\beta}{\beta_0} = \left(\frac{r_{\rm dust}}{r_{\rm 0dust}}\right)^{-1}$$

Kobayashi et al. 2009

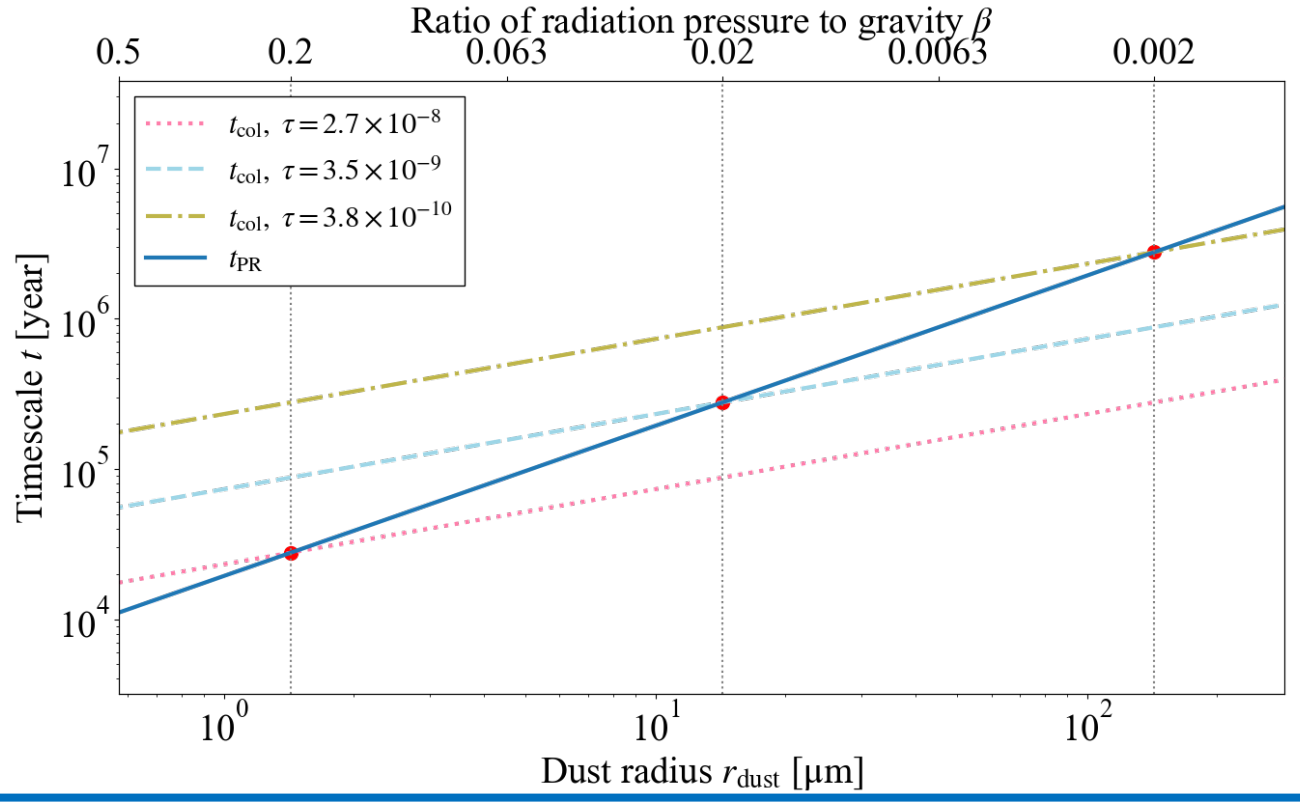

Why eccentricity increases with resonant motion

Ellipse eccentricity e, minor axis a, major axis b, area A

$$b^2 = a^2(1 - e^2)$$

$$A = \pi ab$$

Average motion (angular velocity) n, period T

$$n = \frac{2\pi}{T}$$

Kepler's second law (constant areal velocity)

angular momentum h

$$\frac{\mathrm{d}A}{\mathrm{d}t} = \frac{h}{2}$$

$$\frac{\pi ab}{T} = \frac{h}{2}$$

Kepler's Third Law

$$T^2 = \frac{4\pi^2}{\mu} a^3$$

Squared

$$h^2 = \frac{\mu b^2}{a}$$

$$h = \sqrt{\mu a(1 - e^2)}$$

constant

$$\mu = G(m_1 + m_2)$$

The P-R effect reduces
the angular momentum h.
During resonant motion,
the semi-major axis a remains constant.
Since this is the case,
the eccentricity e increases.

Energy

$$E = -\frac{\mu}{2a}$$ constant

Hermite scheme （Makino & Aarseth 1992）

Acceleration (EoM)

$$\boldsymbol{a}_j = -\sum_{k\neq j} Gm_k \frac{\boldsymbol{r}_{jk}}{r_{jk}^3}$$

Jerk (Time derivative of acceleration)

$$\dot{\boldsymbol{a}}_j = -\sum_{k\neq j} Gm_k \left[\frac{\boldsymbol{v}_{jk}}{r_{jk}^3} - \frac{3(\boldsymbol{v}_{jk}\cdot\boldsymbol{r}_{jk})\boldsymbol{r}_{jk}}{r_{jk}^5}\right]$$

Taylor expansion of acceleration：

$$\boldsymbol{a}_{1,j} = \boldsymbol{a}_{0,j} + \Delta t\dot{\boldsymbol{a}}_{0,j} + \frac{\Delta t^2}{2}\boldsymbol{a}_{0,j}^{(2)} + \frac{\Delta t^3}{6}\boldsymbol{a}_{0,j}^{(3)}$$

solve about $\boldsymbol{a}_{0,j}^{(2)}, \boldsymbol{a}_{0,j}^{(3)}$

$$\dot{\boldsymbol{a}}_{1,j} = \dot{\boldsymbol{a}}_{0,j} + \Delta t\boldsymbol{a}_{0,j}^{(2)} + \frac{\Delta t^2}{2}\boldsymbol{a}_{0,j}^{(3)}$$

Hermite Interpolation

$$\boldsymbol{a}_{0,j}^{(2)} = \frac{-6(\boldsymbol{a}_{0,j} - \boldsymbol{a}_{1,j}) - \Delta t(4\dot{\boldsymbol{a}}_{0,j} + 2\dot{\boldsymbol{a}}_{1,j})}{\Delta t^2}$$

$$\boldsymbol{a}_{0,j}^{(3)} = \frac{12(\boldsymbol{a}_{0,j} - \boldsymbol{a}_{1,j}) + 6\Delta t(\dot{\boldsymbol{a}}_{0,j} + \dot{\boldsymbol{a}}_{1,j})}{\Delta t^3}$$

Hermite scheme（Makino & Aarseth 1992）

- The whole is 4th order accuracy of Δt → The fifth coefficient of Δt is arbitrary

predictor

$$\boldsymbol{x}_{\mathrm{p},j} = \boldsymbol{x}_{0,j} + \Delta t \boldsymbol{v}_{0,j} + \frac{\Delta t^2}{2}\boldsymbol{a}_{0,j} + \frac{\Delta t^3}{6}\dot{\boldsymbol{a}}_{0,j}$$

$$\boldsymbol{v}_{\mathrm{p},j} = \boldsymbol{v}_{0,j} + \Delta t \boldsymbol{a}_{0,j} + \frac{\Delta t^2}{2}\dot{\boldsymbol{a}}_{0,j}$$

corrector

$$\boldsymbol{x}_{\mathrm{c},j}(t+\Delta t) = \boldsymbol{x}_{\mathrm{p},j}(t+\Delta t) + \frac{\Delta t^4}{24}\boldsymbol{a}^{(2)}_{0,j} + \alpha\frac{\Delta t^5}{120}\boldsymbol{a}^{(3)}_{0,j}$$

$$\boldsymbol{v}_{\mathrm{c},j}(t+\Delta t) = \boldsymbol{v}_{\mathrm{p},j}(t+\Delta t) + \frac{\Delta t^3}{6}\boldsymbol{a}^{(2)}_{0,j} + \frac{\Delta t^4}{24}\boldsymbol{a}^{(3)}_{0,j}$$